[redacted]

[redacted]

NACA

RESEARCH MEMORANDUM

FLIGHT MEASUREMENTS OF AVERAGE SKIN-FRICTION COEFFICIENTS ON A PARABOLIC BODY OF REVOLUTION (NACA RM-10) AT MACH NUMBERS FROM 1.0 TO 3.7

By J. Dan Loposer and Charles B. Rumsey

Langley Aeronautical Laboratory
Langley Field, Va.

[redacted]

NATIONAL ADVISORY COMMITTEE
FOR AERONAUTICS

WASHINGTON

August 25, 1954

[redacted]

[redacted]

1D

NACA RM L54G14

NATIONAL ADVISORY COMMITTEE FOR AERONAUTICS

RESEARCH MEMORANDUM

FLIGHT MEASUREMENTS OF AVERAGE SKIN-FRICTION COEFFICIENTS ON A PARABOLIC BODY OF REVOLUTION (NACA RM-10) AT MACH NUMBERS FROM 1.0 TO 3.7

By J. Dan Loposer and Charles B. Rumsey

SUMMARY

Measurements of average skin-friction coefficients have been made on six rocket-powered free-flight models by using the boundary-layer rake technique. The model configuration was the NACA RM-10, a 12.2-fineness-ratio parabolic body of revolution with a flat base.

Measurements were made over a Mach number range from 1 to 3.7, a Reynolds number range from 40×10^6 to 170×10^6 based on length to the measurement station, and with aerodynamic heating conditions varying from strong skin heating to strong skin cooling.

The measurements show the same trends over the test ranges as Van Driest's theory for turbulent boundary layer on a flat plate. The measured values are approximately 7 percent higher than the values of the flat-plate theory.

A comparison which takes into account the differences in Reynolds number is made between the present results and skin-friction measurements obtained on NACA RM-10 scale models in the Langley 4- by 4-foot supersonic pressure tunnel, the Lewis 8- by 6-foot supersonic tunnel, and the Langley 9-inch supersonic tunnel. Good agreement is shown at all but the lowest tunnel Reynolds number conditions.

A simple empirical equation is developed which represents the measurements over the range of the tests.

INTRODUCTION

A considerable portion of the total drag of typical airplane and missile configurations at supersonic speeds is due to skin friction, and the accurate prediction of the skin-friction drag coefficient at supersonic speeds is of importance, especially with regard to the magnitude

of the decrease with increasing Mach number. Several theories predict dissimilar reductions in the skin-friction drag coefficient with increase in Mach number, and experimental data from which the accuracy of the theories can be evaluated are very meager. The effect of aerodynamic heating on the skin-friction coefficient is also predicted to be appreciable. Since airplane and missile flight conditions normally include variable aerodynamic heating conditions, the accuracy of the prediction is important.

In order to provide experimental skin-friction data over a wide range of Mach number, Reynolds number, and aerodynamic heating conditions, the National Advisory Committee for Aeronautics has conducted a rocket-propelled flight test program in which average skin-friction coefficients were measured on a parabolic body of revolution (NACA RM-10) by using the boundary-layer rake technique. The first results of this program were published in reference 1. Several additional flight tests have been conducted which refined the instrumentation and extended the range of the test conditions. Results of these tests are reported herein. The Mach number range covered was from 1.0 to 3.7, the Reynolds number range (based on body length to the measurement station) was from 40×10^6 to 170×10^6, and the aerodynamic heating conditions varying from strong skin heating to strong skin cooling. The tests were conducted at the Langley Pilotless Aircraft Research Station at Wallops Island, Va.

SYMBOLS

C_f	average skin-friction coefficient based on wetted area ahead of measurement station
$C_{f_{emp}}$	average skin-friction coefficient computed from empirical formula
C_{f_i}	incompressible average skin-friction coefficient
$C_{f_{meas}}$	measured values of average skin-friction coefficient from present investigation, based on area ahead of measurement station
$C_{f_{Van\ Driest}}$	average skin-friction coefficient computed from Van Driest's theory
h	altitude, ft
M	Mach number
M_δ	Mach number at outer edge of boundary layer

R_x	Reynolds number based on axial distance from nose of model
t	time, sec
T	temperature, ^{o}F abs.
T_{aw}	adiabatic wall temperature, ^{o}F abs.
T_w	representative temperature of skin ahead of measurement station, ^{o}F abs.
y	distance normal from skin, in.
ϕ	wall heating parameter, $\frac{T_{aw} - T_w}{T_{aw} - T_l}$

Subscripts:

l	free-stream conditions

MODELS AND TESTS

Figure 1 shows the dimensions of the models tested, and figure 2 is a photograph of a model and its booster on the launcher. The model configuration is designated NACA RM-10. The body is a parabolic body of revolution with a basic fineness ratio of 15. An actual fineness ratio of 12.2 results from cutting off the rear portion to form a base area for rocket exhaust. The body is 146.5 inches long with a 12-inch maximum diameter. Four fins are equally spaced around the base. They are untapered, have 60° sweepback, and have a 10-percent-thick circular-arc profile normal to the leading edge. The models were constructed of magnesium alloy except for a steel tip on the nose and steel leading and trailing edges on the fins, which were necessary to prevent melting of the needle point and knife edges. The cast fins were welded to the cast rear section of the body. The body ahead of the fin section was spun from 0.09-inch-thick magnesium, with a 6-inch solid-magnesium nosepiece.

Six joints were necessary for the construction and assembly of the model, three of these being permanent joints. The steel tip was pressed permanently on the solid-magnesium nose which was fastened permanently to the spun-magnesium body at station 6. A permanent riveted joint was located at station 90, the station of maximum diameter. These permanent joints were very carefully handworked and polished to make the surface

juncture as smooth as possible. Threaded joints were located at stations 23, 80, and 125. These joints were very carefully constructed and fitted, but surface discontinuities of the order of 0.005 inch at the station-80 joint could not be eliminated because of the large diameter and thin wall construction. Stiffening rings were located only at the joints of stations 23, 80, 90, and 125, and these were designed to prevent changes in body contour due to the expansion caused by aerodynamic heating. The contour of the finished models varied from the design dimensions by a maximum of 0.25 percent of the local diameter, and the surface roughness, except for joints, was less than 60 microinches from peak to valley as measured with a Brush surface analyzer with a 0.0005-inch-radius stylus.

ABL Deacon rocket motors which have a total impulse of approximately 18,400 pound-seconds were used for propulsion. A booster consisting of two Deacon motors burning simultaneously accelerated the model to a Mach number of approximately 2.0. At burnout of the booster rocket motor, the booster drag-separated and the model coasted for a predetermined time before ignition of the internally carried Deacon sustainer motor which accelerated the model to maximum Mach number. Data were telemetered from the model continuously and were automatically recorded at two ground receiving stations. The models were tracked by a CW Doppler velocimeter from take-off until approximately 5 seconds after maximum Mach number. The velocity time history thus obtained was extended by integration of the telemetered accelerations. Position of the model in space was obtained from an SCR 584 radar tracking unit. Atmospheric data were measured by means of radiosondes, which were automatically tracked by radar to supply wind velocity and direction at altitudes. Figure 3 is a drawing of the boundary-layer total-pressure rake which was used to measure the average skin-friction coefficients for the body ahead of the rake station. Figure 4 is a photograph of the rake installation on model 4. Six models were flight tested in the present investigation. The rake was mounted at station 125 on models 1 to 5 and at station 85 on model 6. Figure 5 shows typical time histories of altitude, aerodynamic heating parameter, Reynolds number, and Mach number for the tests. Only the trajectory for model 5 differs significantly from the example. The first coast period for model 5 ended at approximately 8 seconds resulting in higher Reynolds numbers at comparable Mach numbers. Also shown is a curve of skin-friction coefficient computed for the test conditions shown using Van Driest's flat-plate turbulent boundary-layer theory (ref. 2). During the first coast after booster separation, Mach number and Reynolds number decrease as the model slows down. Since the skin temperature has not yet reached adiabatic wall temperature at booster separation, the temperature parameter $\frac{T_{aw} - T_w}{T_{aw} - T_l}$ is positive at the beginning of the coast period. The decreasing speed during coast causes T_{aw} to decrease. Wall temperature, however, is increasing because of aerodynamic heating and at approximately

[redacted]

midway of the coast they become equal, making the temperature parameter equal to zero. Wall temperature then begins to decrease, lagging T_{aw}, and the temperature parameter becomes negative. During power on, T_{aw} increased and became much higher than T_w, thus causing the temperature parameter to again become positive. During the second coast, a sequence of temperature variations occurs similar to that during the first coast.

ANALYSIS

Average skin-friction drag coefficients were determined on the NACA RM-10 body by means of total-pressure rake surveys through the boundary layer and measurements of the static pressure and skin temperature at the measurement station. The total-pressure and static-pressure measurements were used to obtain Mach numbers from which Mach number profiles through the boundary layer were obtained by fairing. Figure 6 shows three typical Mach number profiles from model 5 plotted as M/M_δ against distance from skin. The measured points are shown by symbols. The symbols are shown at the y distance corresponding to the geometric center of the tube. Some investigations have indicated that the geometric center of the total-pressure probe does not correspond to the effective center of pressure when measurements are made in a pressure gradient across the tube mouth. An estimate for conditions of the present tests indicates the shift to be negligible. The Mach number profiles were used along with the equation for the temperature distribution through the boundary layer, which was given by Crocco in reference 3, to obtain velocity and density profiles through the boundary layer. The velocity and density profiles were then used in the momentum equation to obtain average skin-friction drag coefficients for the area ahead of the measurement station. The reduction procedure for the data reported herein is the same as that described in greater detail in reference 1, except for the value of the temperature recovery factor inserted in the Crocco temperature equation. In reference 3 a temperature recovery factor of 0.88 was used, whereas in the present report a value of 1.0 was used. Although the value of 0.88 satisfies the boundary condition for temperature of the skin at equilibrium, the value of 1.0 was found to give better agreement of temperature profiles within the boundary layer when compared with profiles calculated by using measured variations of recovery factor within the boundary layer from reference 4. For the conditions calculated for comparison, the effect of changing the recovery factor from 0.88 to 1.0 amounted to less than 2-percent change in average skin-friction coefficient.

In the present paper the wall heating condition is expressed by a dimensionless temperature parameter ϕ which is defined as $\phi = \frac{T_{aw} - T_w}{T_{aw} - T_l}$.

This parameter, which is the ratio of the temperature difference between the adiabatic wall temperature and the actual skin temperature to the temperature rise which would be attained on an insulated wall, has the added significance of indicating geometrically similar nondimensional boundary-layer temperature profiles for equal values of ϕ. A complete derivation and discussion of this parameter is given in the appendix of reference 5. The value of T_w used in the parameter was taken as the temperature of the skin at the average area station ahead of the rake. This is the station which divides the model surface area ahead of the measurement station in half. Skin temperature measurements made at several stations on the NACA RM-10 body during test trajectories similar to those herein show that the temperature is not constant along the skin, with a maximum difference of 180° F between stations 18 and 122 occurring shortly after peak Mach number. The skin temperature at the average area station is believed to represent best the heating condition affecting C_f.

RESULTS AND DISCUSSION

Presentation of Results

Shown in figure 7 are plots of average skin-friction coefficients, Reynolds number, and temperature parameter against Mach number for each of the six models. Models 1 to 4 all had a similar delay time (first coast) of approximately 10 seconds. The curves of Reynolds numbers for these models show that similar ranges of Reynolds number were covered during first coast, power on and second coast, with considerably different Mach numbers occurring at comparable Reynolds numbers. The Reynolds number variation of model 5 was similar to that of models 1 to 4 except that a slightly higher Reynolds number was attained at peak Mach number because of its shorter delay time of 5 seconds which caused its maximum Mach number to occur at a lower altitude. The Reynolds numbers of model 6 were proportionately lower than those of models 1 to 4 as a result of having its measurement station at 85 inches instead of 125 inches as on the other models.

The temperature parameter for models 1 to 4 covered a similar range during first coast, power on and second coast. The temperature parameter for model 5 differed only in that it did not become negative during the first coast because of its shorter delay time.

The measured average skin-friction coefficients are shown in figure 7 along with a curve of Van Driest's theory for turbulent skin-friction on a flat-plate at the test conditions of Mach number, Reynolds number, and skin temperature. The experimental points show a change in skin-friction coefficient of from 30 to 40 percent over the test range.

Van Driest's theory for skin friction on a smooth flat plate, computed for the test conditions, shows a very similar trend.

Comparison With Flat-Plate Theory

A comparison of the measured skin-friction coefficients from the NACA RM-10 body with the flat-plate theory is made in figure 8 by plotting one against the other. Data are shown for the five models on which measurements were made at station 125. The dashed line, faired through the data points, is 7 percent above the line representing $C_{f_{meas}} = C_{f_{Van\ Driest}}$. The band drawn ±5 percent about the faired line includes 66 percent of the points. Although there is scatter in the data when plotted in this manner, reference to figure 7 shows that the cause is not random scatter in measurements from an individual model but is the difference in the agreement between measurement and theory from model to model. The reason for this variation in agreement at similar test conditions is not understood. A possible cause may be very small model flight trim angles. Reference 6 shows small differences between boundary-layer profiles measured at diametrically opposite points on a body of revolution in a wind tunnel. The difference is attributed to very small misalinement (a few tenths of a degree) of the model axis with the undisturbed stream direction. Similarly, in the present tests, small misalinement of the fins may have caused the models to trim at a very small angle of attack.

Although the extent of laminar boundary layer which may have existed over the nose of the body is not known, the data are compared with theory for fully turbulent flow over the model. Three reasons to believe the comparison is valid are as follows: (1) skin-temperature measurements made at station 18 on the NACA RM-10 body show turbulent heat-transfer coefficients at this station at all times during test trajectories similar to those herein; (2) calculations, based on consideration of the small area of the nose under laminar flow and the shortening of the effective length of turbulent run, indicate that laminar flow back to station 20 would cause only a 1.5-percent reduction in the measured average skin-friction coefficient; and (3) the level of the agreement with theory does not change between the data taken at the highest Reynolds numbers and the lowest. If the length of laminar flow increased significantly at the lower Reynolds numbers, the level of the data would have been lowered. At the higher Reynolds number conditions, transition must occur ahead of station 20 or the transition Reynolds number would be unreasonably high.

Figure 9 shows the data from rakes at station 85 from model 6 of the present tests and from model 2 of reference 1 plotted against $C_{f_{Van\ Driest}}$ for the flight test conditions. The data from reference 1 are approximately 10 percent higher than the data from model 6 which scatter about the level of the Van Driest theory. No conclusion is drawn from the limited data from these two models.

[redacted]

Comparison With Tunnel Measurements

Skin-friction measurements have been obtained on the NACA RM-10 body shape in the Langley 4- by 4-foot supersonic pressure tunnel (ref. 7), the Lewis 8- by 6-foot supersonic tunnel (ref. 8), and the Langley 9-inch supersonic tunnel (ref. 9) by both the boundary-layer rake technique and the drag-component technique. Reference 10 presents a compilation of these data from Mach numbers of 1.49 to 2.41 and at Reynolds numbers below 40×10^6. The turbulent skin-friction data of reference 10 are used for comparison with the results of the present investigation. However, it was necessary to convert the skin-friction coefficients from the present investigation to the Reynolds number and zero heating condition for which the tunnel data were obtained.

In order to evaluate the effect of Mach number, skin-friction coefficients were read for models 1 to 5 from figure 7 at the condition of zero heating. These values were divided by the incompressible skin-friction coefficient for the same Reynolds number and were plotted against Mach number in figure 10. The incompressible values of C_f were obtained from reference 11 which reports incompressible C_f measurements on the full-scale NACA RM-10 body from towing tank tests. The results from reference 11 show that the incompressible C_f on the NACA RM-10 body agrees with the Von Kármán-Schoenherr curve (ref. 12) for C_{f_i}. Also shown in figure 10 is the variation of C_f/C_{f_i} given by Van Driest's theory at Reynolds numbers of 10, 60, and 170×10^6. These theoretical lines show that this wide range of Reynolds number modifies the relation of C_f/C_{f_i} with Mach number by only 6 percent at a Mach number of 3, and less at lower Mach numbers. Most of the experimental points on figure 10 are for a Reynolds number of approximately 60×10^6. The theoretical curves for 170×10^6 and 10×10^6 are shown since they cover the upper limit of the present data and the lower limit of the tunnel data used for comparison. As in figure 8, the line representing the fairing of the data is approximately 7 percent above Van Driest's theory at the corresponding Reynolds number (60×10^6).

Figure 10 is used to convert the results of the present investigation for comparison with the tunnel data of reference 10. Values of C_f/C_{f_i} were read from the experimental curve at the tunnel Mach number, and multiplied by C_{f_i} at the tunnel Reynolds number. Van Driest's theory curves indicate a maximum correction of 2.5 percent to the C_f/C_{f_i} values because of the Reynolds number differences between the experimental curve and the tunnel tests. These small corrections were made.

The comparison of the data from this investigation, converted as indicated, with the tunnel data is shown in figure 11. Figure 11(a) shows the comparison with data from the Langley 4- by 4-foot supersonic pressure tunnel and the Langley 9-inch supersonic tunnel at a Mach number of 1.6 over a range of Reynolds number. Tunnel measurements are shown for conditions of natural transition and for transition fixed near the nose. For natural transition, C_f is low at the low Reynolds numbers because of the greater proportion of laminar flow over the body. Results of the present tests are in very good agreement with the natural transition tunnel data above a Reynolds number of 32×10^6. The agreement with the fixed transition data is very good at $R_x = 28 \times 10^6$ and is within 8 percent at the lower Reynolds numbers. Figure 11(b) shows the comparison with the results from tests in the Lewis 8- by 6-foot supersonic tunnel for $R_x \approx 30 \times 10^6$ over a Mach number range from 1.49 to 1.98. The difference is less than 4 percent. Figure 11(c) shows the comparison with data from the Langley 9-inch supersonic tunnel for $R_x = 8.5 \times 10^6$ at Mach numbers from 1.62 to 2.41. The tunnel model had transition fixed near the nose and the tunnel data are from 5 to 13 percent below the data from the present investigation. In summary, the comparison of the present data with that from the three tunnels shows good agreement at all but the lowest Reynolds numbers.

Development of Empirical Equation

In order to define the effects of heating on the measured skin friction, values of C_f/C_{f_i} have been plotted against Mach number in figure 12 for several values of heating parameter. Values of C_f were read from a fairing of C_f data from figure 7 for constant values of ϕ and were divided by C_{f_i} for the same Reynolds number. In figure 12(a), the experimental curve for zero heating from figure 10 is reproduced and a straight-line fairing is shown as an alternate fairing above $M = 1.0$. Figures 12(b), (c), and (d) show points taken from a fairing of the C_f data from figure 7 at constant values of the heating parameter ϕ with a straight line fairing drawn to represent the points. For any specific value of the temperature parameter the fairing does not in all cases appear to be the best possible one; however, the trends of the data points with variation of the heating parameter seem to justify the family of curves obtained from figure 12.

The empirical formula for the variation of C_f/C_{f_i} as obtained from the straight-line fairings of figure 12 is

$$\frac{C_f}{C_{f_i}} = \left(0.075 \frac{T_{aw} - T_w}{T_{aw_i} - T_l} - 0.15\right)(M - 1.0) + 1.0.$$

The value of C_{f_i} may be selected from a plot of the Kármán-Schoenherr equation $\left(\text{i.e., } \frac{0.242}{\sqrt{C_f}} = \log_{10} R_x C_f\right)$ at the value of Reynolds number for computation of C_f, or the equation $C_{f_i} = \frac{0.0277}{R_x^{0.1405}}$, which represents the Kármán-Schoenherr equation within 1 percent from $R_x = 20 \times 10^6$ to 200×10^6, may be substituted in the empirical formula. The resultant empirical equation then becomes

$$C_f = \frac{0.0277}{R_x^{0.1405}}\left[\left(0.075\,\frac{T_{aw} - T_w}{T_{aw} - T_l} - 0.15\right)(M - 1) + 1.0\right]$$

The empirical equation is valid only between Mach numbers 1.0 and 3.5. Values of C_f greater than C_{f_i} would result if used for Mach numbers from 0 to 1.0. The empirical equation is presented primarily to show the grouping of parameters in a comparatively simple form which represents the present data within the accuracy of the measurements.

Comparison of Data With Empirical Equation

Figure 13 shows the present data plotted against the values of C_f from the empirical equation. The line expressing $C_{f_{meas}} = C_{f_{emp}}$ constitutes a good fairing of the data. Since a ±5-percent band includes 66 percent of the experimental points, the empirical equation is believed to be a good representation of the measurements. Also shown in figure 13 are data from references 1 and 5. Data from reference 1 are from rake data at station 125 on two NACA RM-10 flight models and are as much as 25 percent higher than the faired line of the present data. No good explanation for this difference has been found, although contributing causes may be the possibility of small angle of attack as mentioned previously and the fact that the models reported in reference 1 were the first flight models using the rake technique which was improved in several small details in later models. The data from reference 5 are from rake data at station 124 on one RM-10 flight model and agrees within 5 percent with the present data. The agreement of the present data is similar to that shown in figure 8 between the data points and the line 7 percent above Van Driest's theory. The reason for this is shown in figure 14 where $C_{f_{emp}}$ is plotted against $C_{f_{Van\ Driest}}$. The points shown are computed for the experimental conditions of two models which were typical

of the present tests. The points lie within ±2 percent of the line $C_{f_{emp}} = 1.07 C_{f_{Van\ Driest}}$.

CONCLUSIONS

Flight tests of six full-scale NACA RM-10 rocket-propelled models have been conducted for measurement of average skin-friction coefficients. Measurements were made over a Mach number range from 1.1 to 3.7, a Reynolds number range from 40×10^6 to 170×10^6, and with aerodynamic heating conditions varying from strong skin heating to strong skin cooling. The following conclusions are presented:

1. Over the conditions of the tests, the measured values show the same trends as Van Driest's flat-plate turbulent theory. The measured values are approximately 7 percent higher than Van Driest's theory.

2. By plotting the data as the ratio of average skin-friction coefficient C_f to the incompressible average skin-friction coefficient C_{f_i} and utilizing the experimental curve of C_{f_i} obtained for the NACA RM-10 body in NACA Rep. 1161, a comparison is made between the present results and skin-friction measurements obtained on RM-10 scale models in the Langley 4- by 4-foot supersonic pressure tunnel, the Lewis 8- by 6-foot supersonic tunnel, and the Langley 9-inch supersonic tunnel. Agreement at tunnel Reynolds numbers from 25×10^6 to 40×10^6 was good and at Reynolds numbers from 8×10^6 to 25×10^6 the agreement with tunnel measurements, for transition fixed near the nose, was within 13 percent.

3. A simple empirical equation was developed from the data to represent the measurements over the range of the tests.

Langley Aeronautical Laboratory,
National Advisory Committee for Aeronautics,
Langley Field, Va., June 29, 1954.

[redacted]

REFERENCES

1. Rumsey, Charles B., and Loposer, J. Dan: Average Skin-Friction Coefficients From Boundary-Layer Measurements in Flight on a Parabolic Body of Revolution (NACA RM-10) at Supersonic Speeds and at Large Reynolds Numbers. NACA RM L51B12, 1951.

2. Van Driest, E. R.: The Turbulent Boundary Layer for Compressible Fluids on a Flat Plate With Heat Transfer. Rep. No. AL-997, North American Aviation, Inc., Jan. 27, 1950.

3. Crocco, Luigi: Transmission of Heat From a Flat Plate to a Fluid Flowing at a High Velocity. NACA TM 690, 1932.

4. Spivack, H. M.: Experiments in the Turbulent Boundary Layer of a Supersonic Flow. Rep. No. CM-615, North American Aviation, Inc., Jan. 16, 1950.

5. Maloney, Joseph P.: Drag and Heat Transfer on a Parabolic Body of Revolution (NACA RM-10) in Free Flight to Mach Number 2 With Both Constant and Varying Reynolds Number and Heating Effects on Turbulent Skin Friction. NACA RM L54D06, 1954.

6. Chapman, Dean R., and Kester, Robert H.: Turbulent Boundary-Layer and Skin-Friction Measurements in Axial Flow Along Cylinders at Mach Numbers Between 0.5 and 3.6. NACA TN 3097, 1954.

7. Czarnecki, K. R., and Marte, Jack E.: Skin-Friction Drag and Boundary-Layer Transition on a Parabolic Body of Revolution (NACA RM-10) at a Mach Number of 1.6 in the Langley 4- by 4-Foot Supersonic Pressure Tunnel. NACA RM L52C24, 1952.

8. Esenwein, Fred T., Obery, Leonard J., and Schueller, Carl F.: Aerodynamic Characteristics of NACA RM-10 Missile in 8- by 6-Foot Supersonic Wind Tunnel at Mach Numbers From 1.49 to 1.98. II - Presentation and Analysis of Force Measurements. NACA RM E50D28, 1950.

9. Love, Eugene S., Coletti, Donald E., and Bromm, August F., Jr.: Investigation of the Variation With Reynolds Number of the Base, Wave, and Skin-Friction Drag of a Parabolic Body of Revolution (NACA RM-10) at Mach Numbers of 1.62, 1.93, and 2.41 in the Langley 9-Inch Supersonic Tunnel. NACA RM L52H21, 1952.

10. Evans, Albert J.: The Zero-Lift Drag of a Slender Body of Revolution (NACA RM-10 Research Model) As Determined From Tests in Several Wind Tunnels and in Flight at Supersonic Speeds. NACA TN 2944, 1953.

11. Mottard, Elmo J., and Loposer, J. Dan: Average Skin-Friction Drag Coefficients From Tank Tests of a Parabolic Body of Revolution (NACA RM-10). NACA Rep. 1161, 1954. (Supersedes NACA TN 2854.)

12. Von Kármán, Th.: Turbulence and Skin Friction. Jour. Aero. Sci., vol. 1, no. 1, Jan. 1934, pp 1-20.

[redacted]

[redacted]

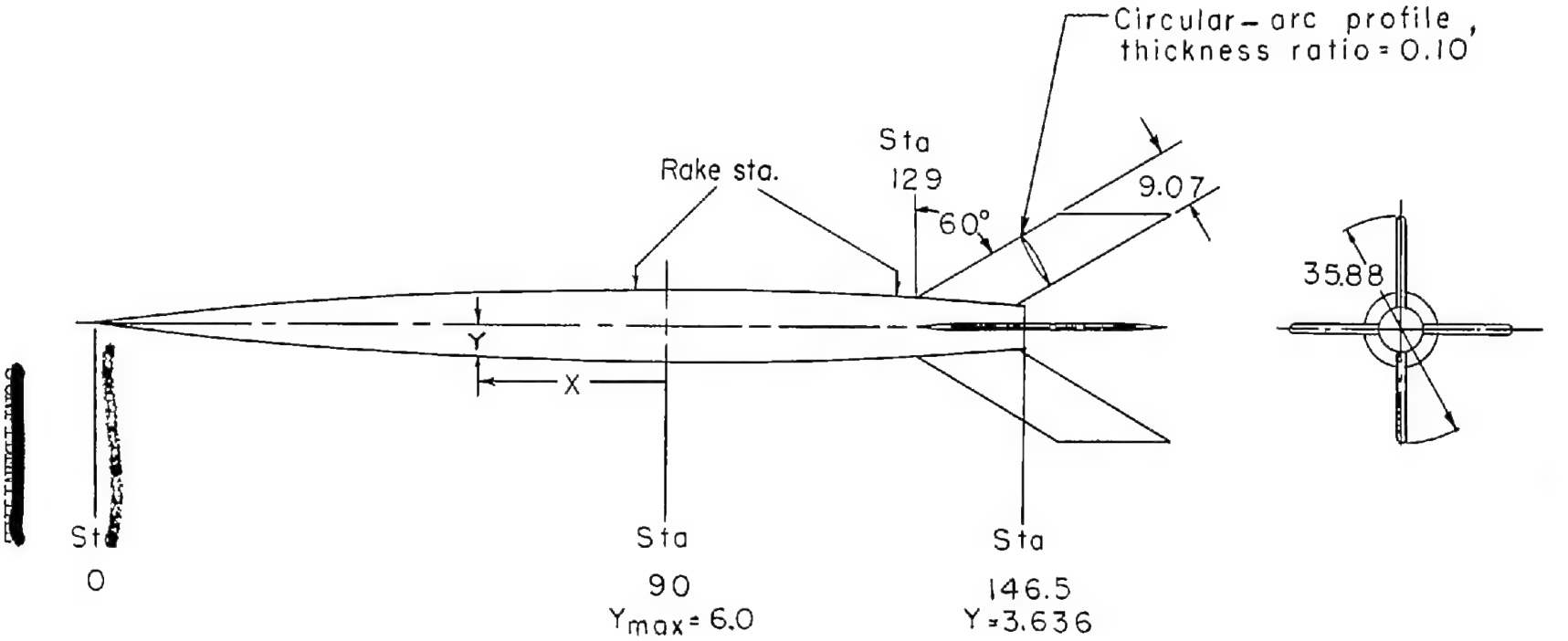

Body profile equation

$$Y = 6.000 - .0007407\,X^2$$

Station number denotes axial distance from nose in inches.

Figure 1.- General configuration and body equation of NACA RM-10 model. Dimensions are in inches.

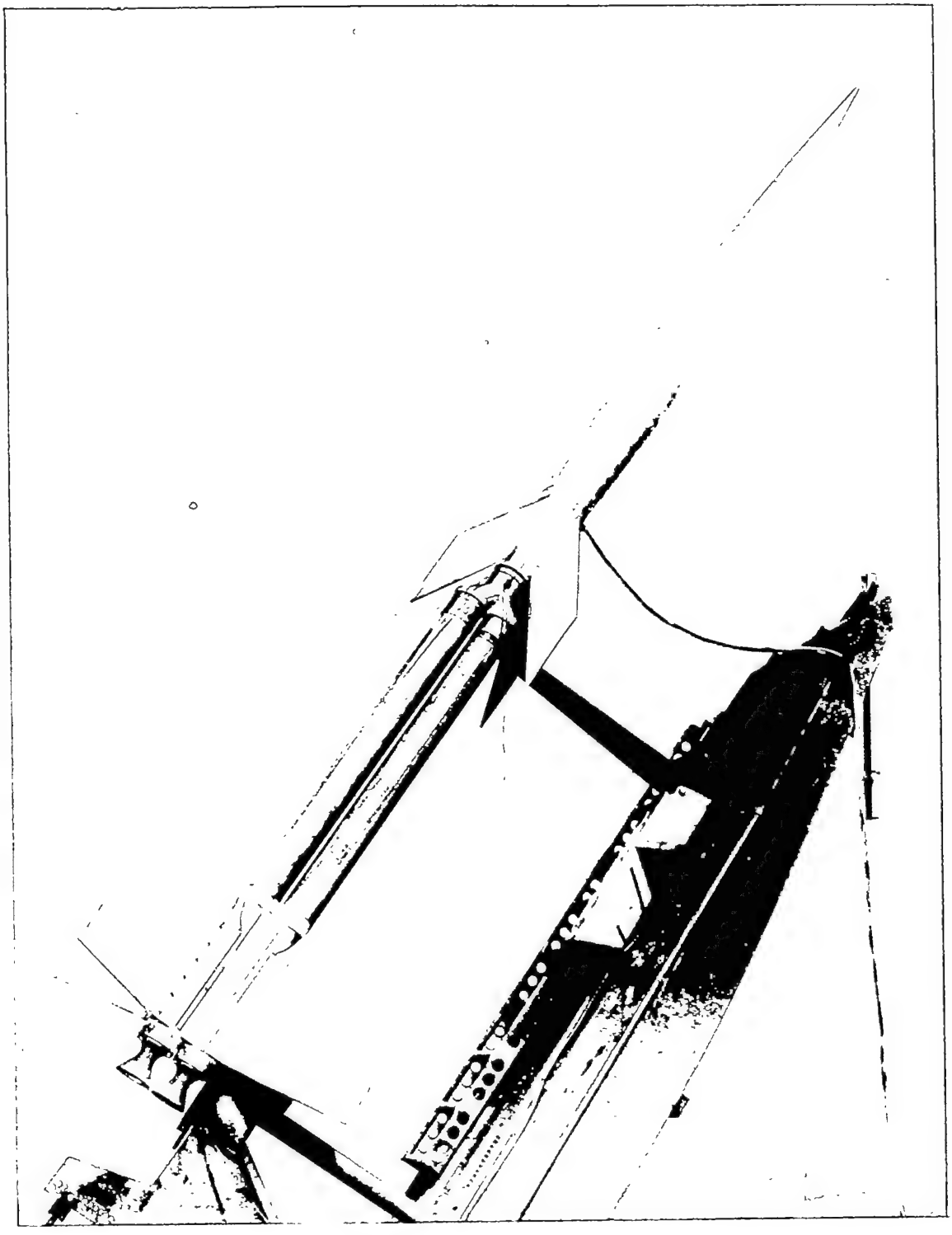

L-70979

Figure 2.- Model 2 in launching position.

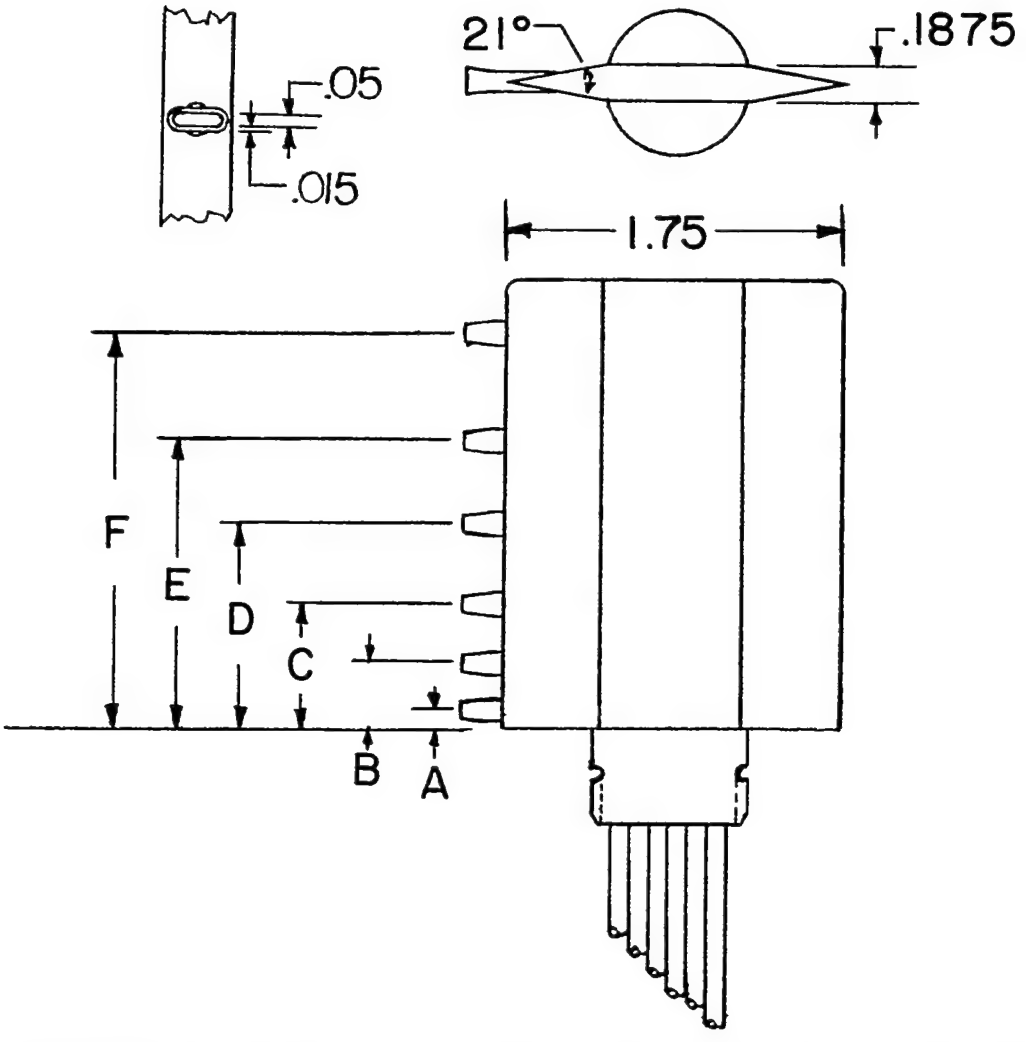

model / tube	1	2	3	4	5	6
A	.055	.065	.100	.048	.050	.050
B	.353	.352	.230	.355	.200	.145
C	.659	.658	.460	.645	.445	.300
D	1.155	1.170	.810	1.145	790	.445
E	1.763	1.760	1.260	1.740	1.245	.640
F	2510	2.507	1.810	2.478	1.785	.900

Figure 3.- Drawing of boundary-layer total-pressure rake. Dimensions are in inches.

Figure 4.- Rake installation on model 4. L-69521

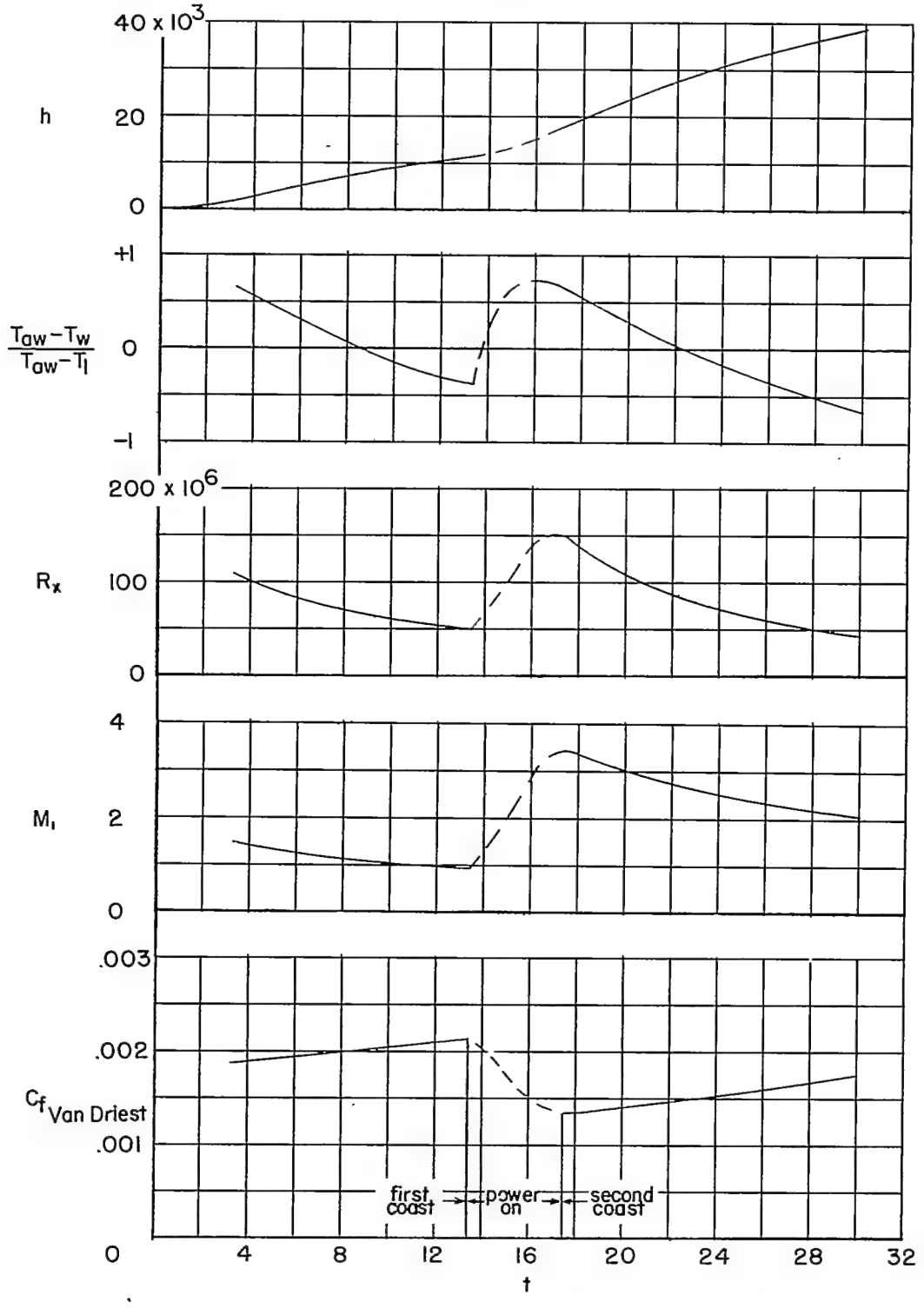

Figure 5.- Time histories of test conditions and predicted average skin-friction coefficients for model 1.

[redacted]

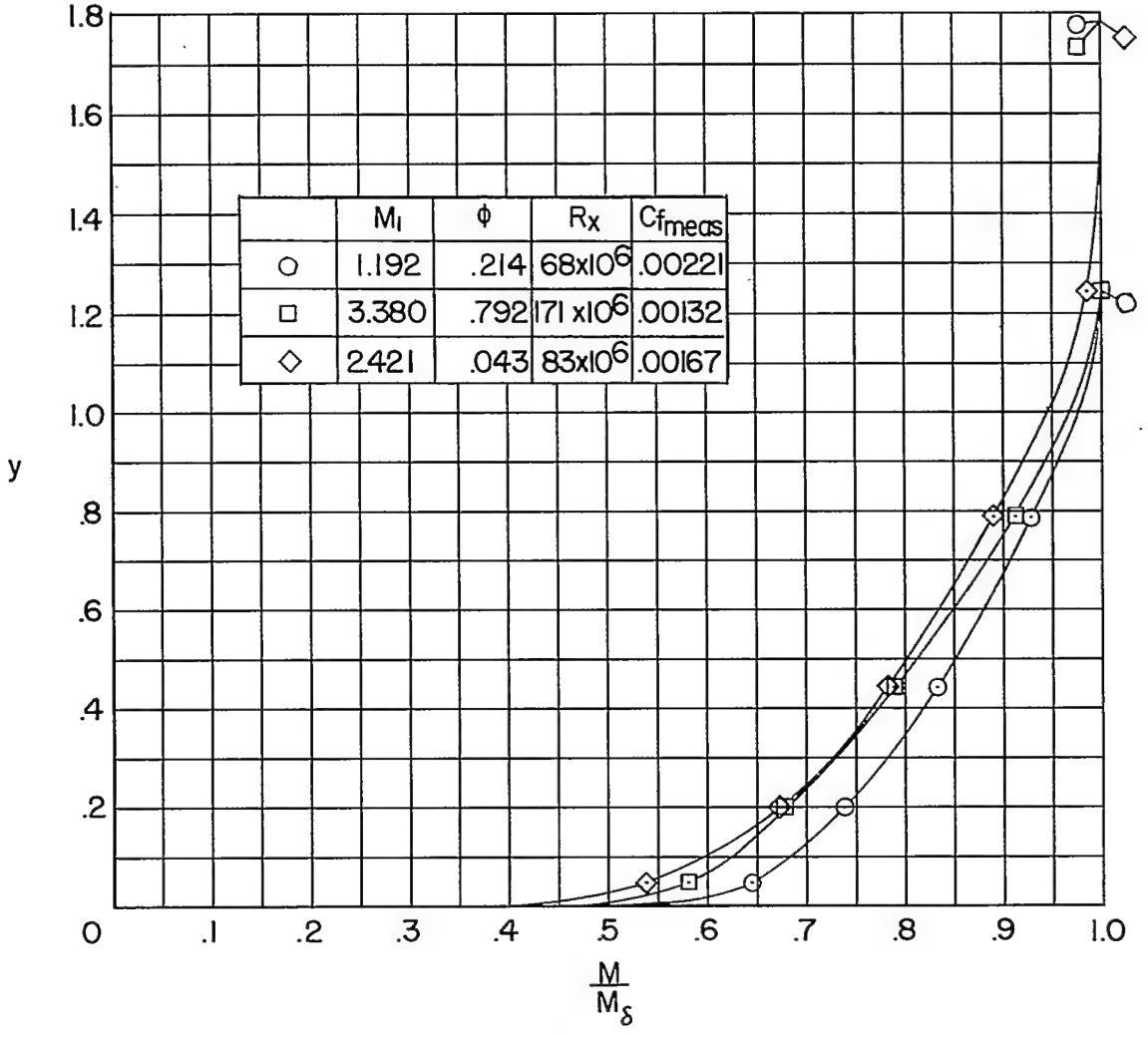

Figure 6.- Mach number profiles from model 5 at three Mach numbers.

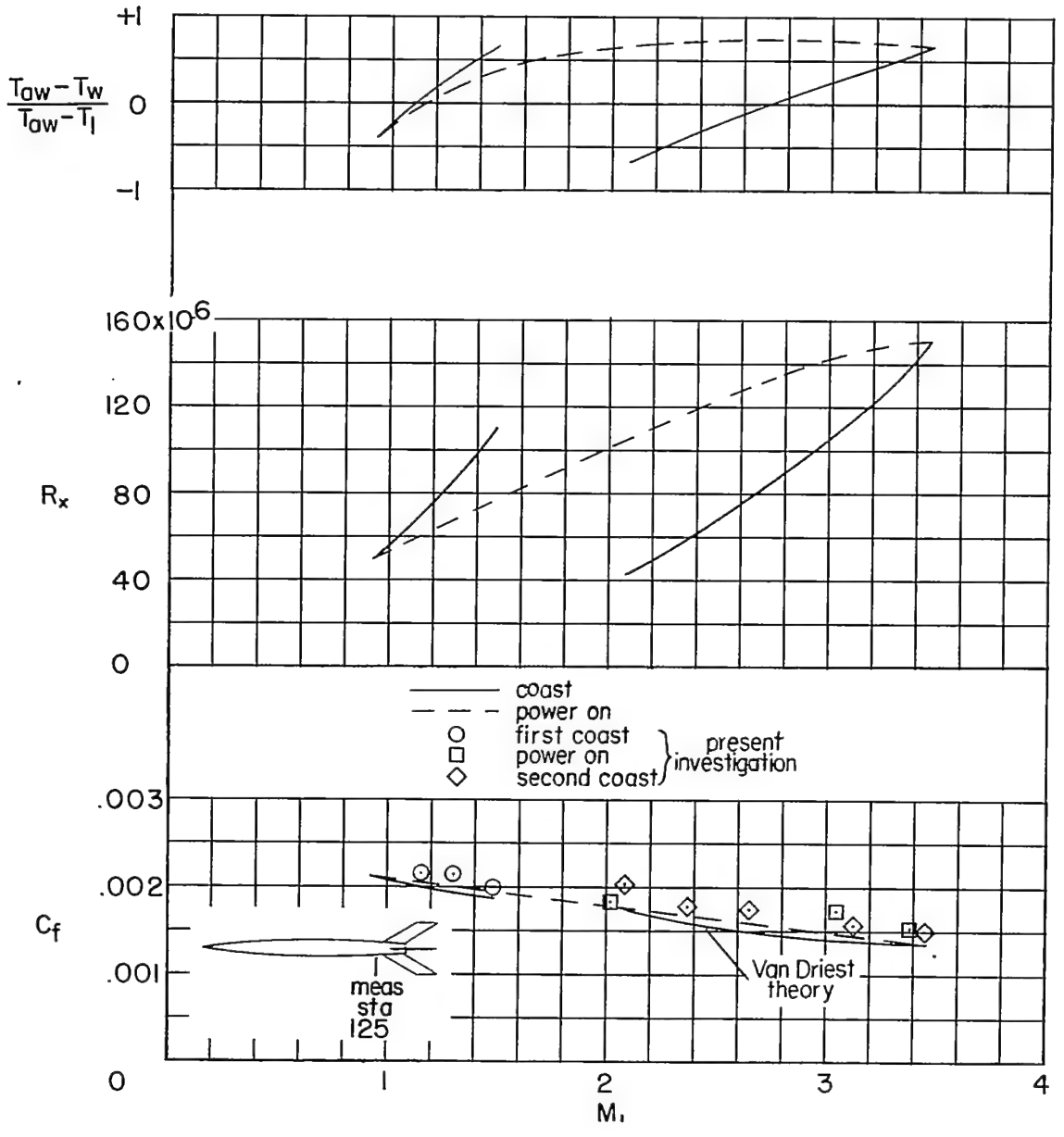

(a) Model 1.

Figure 7.- Average skin-friction coefficients and test conditions plotted against Mach number.

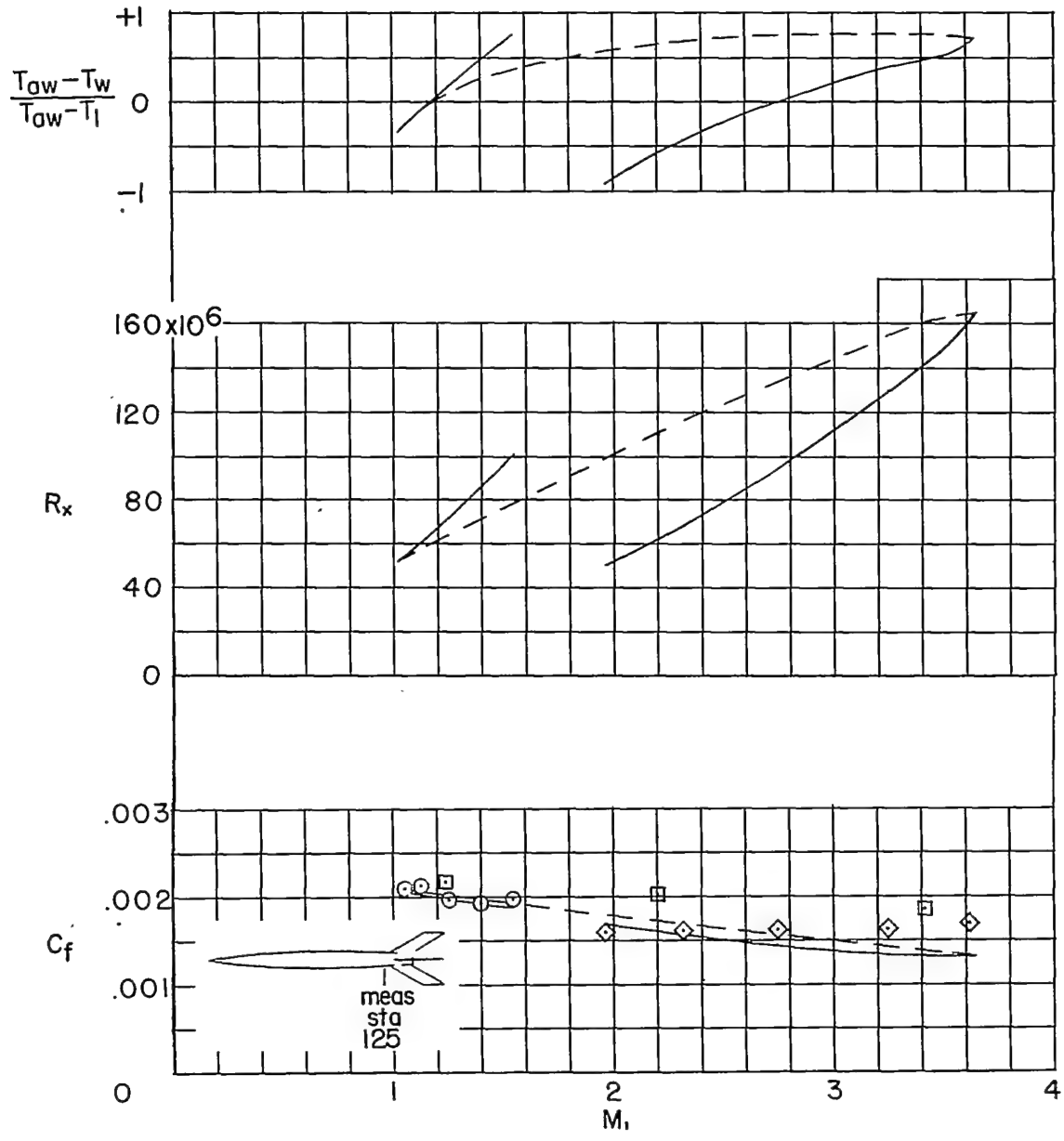

(b) Model 2.

Figure 7.- Continued.

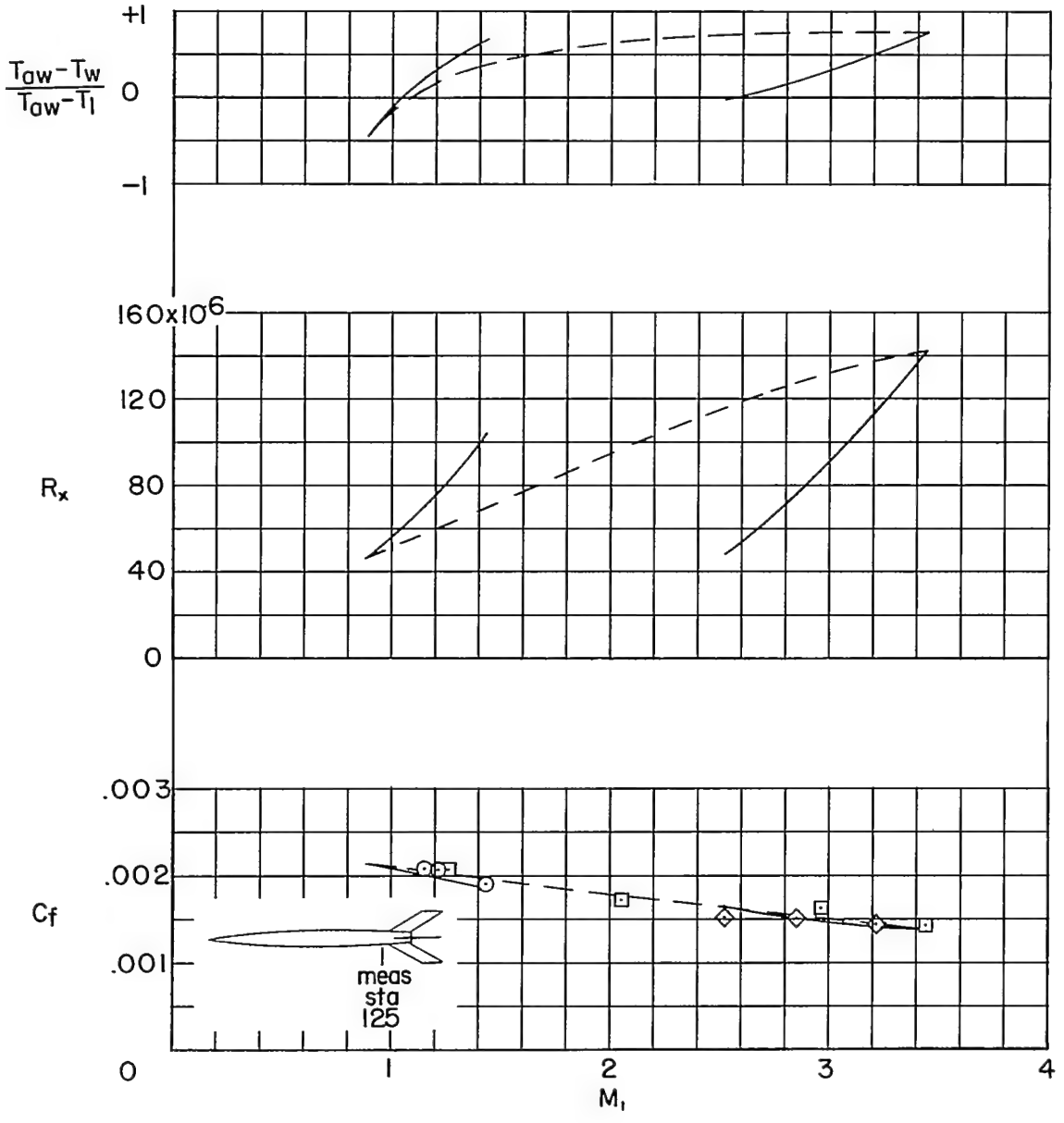

(c) Model 3.

Figure 7.- Continued.

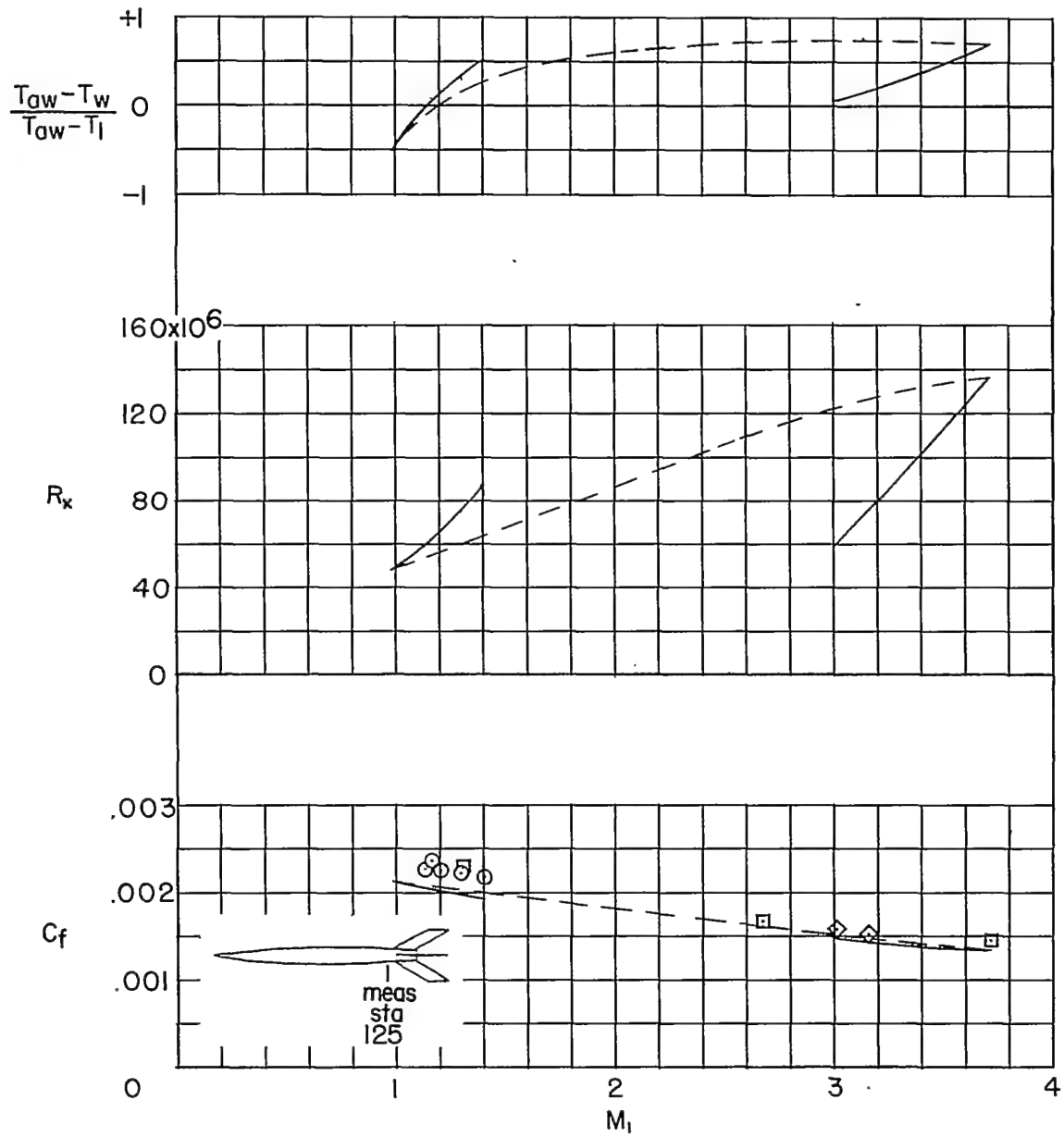

(d) Model 4.

Figure 7.- Continued.

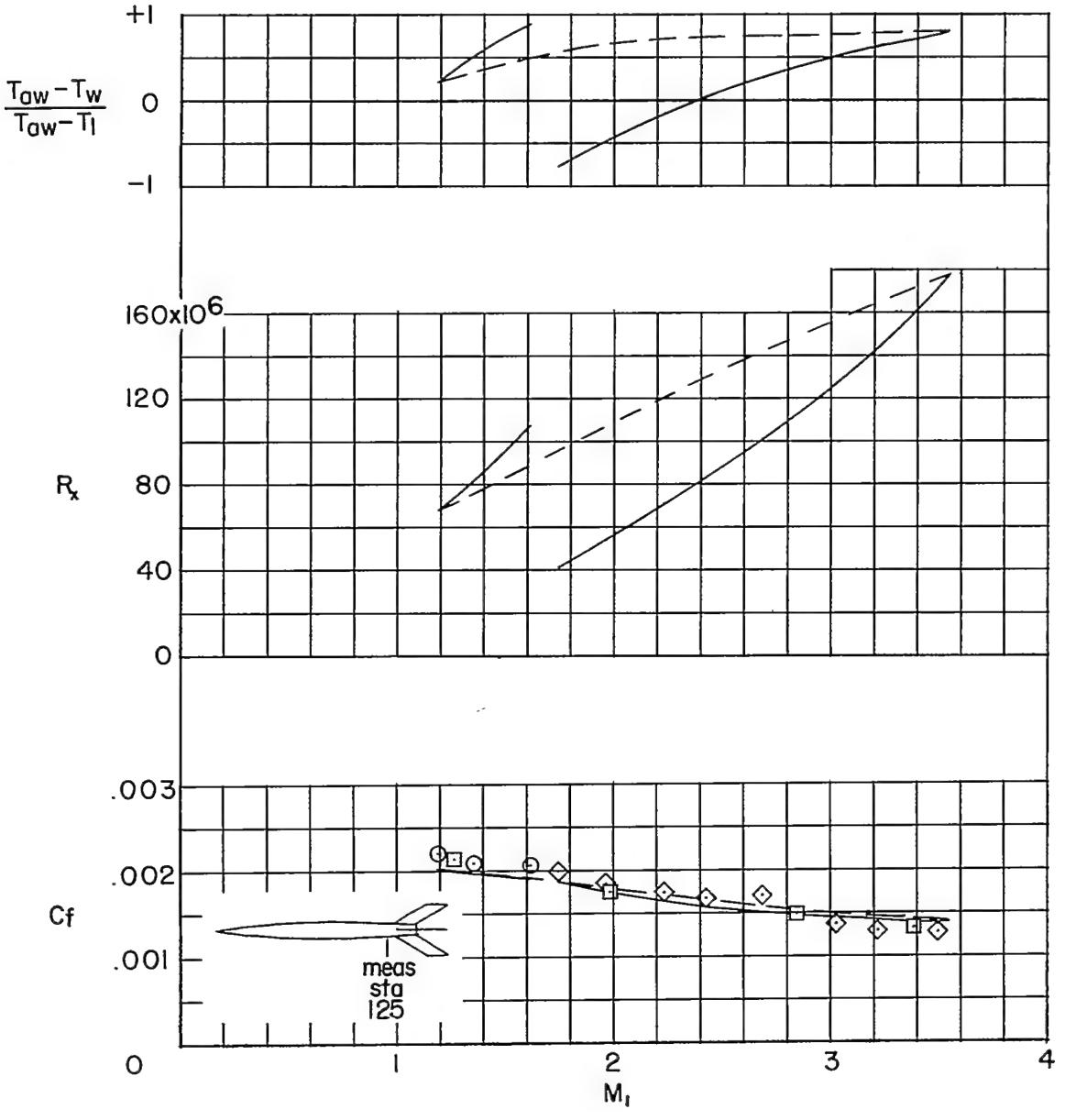

(e) Model 5.

Figure 7.- Continued.

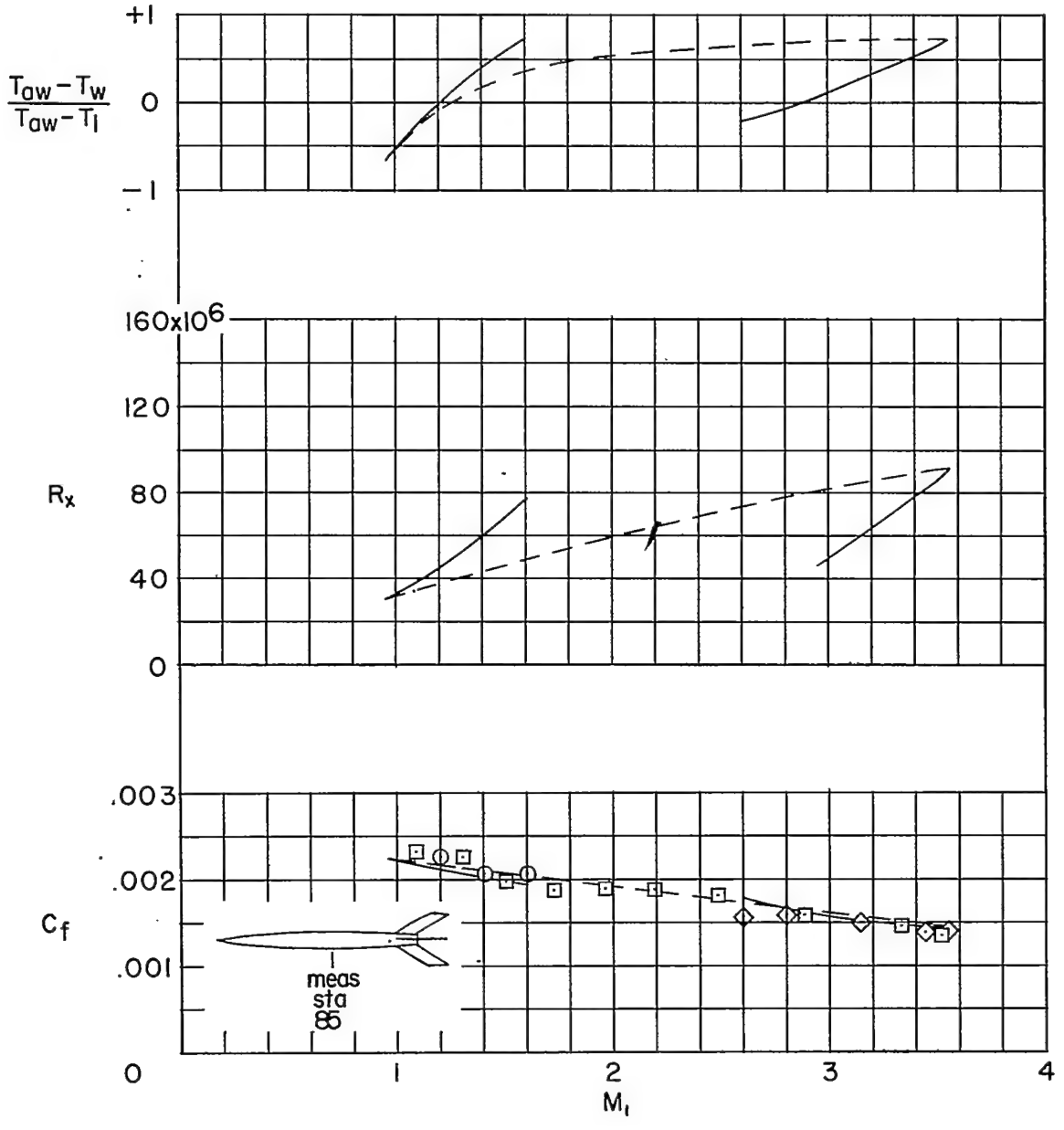

(f) Model 6.

Figure 7.- Concluded.

[redacted]

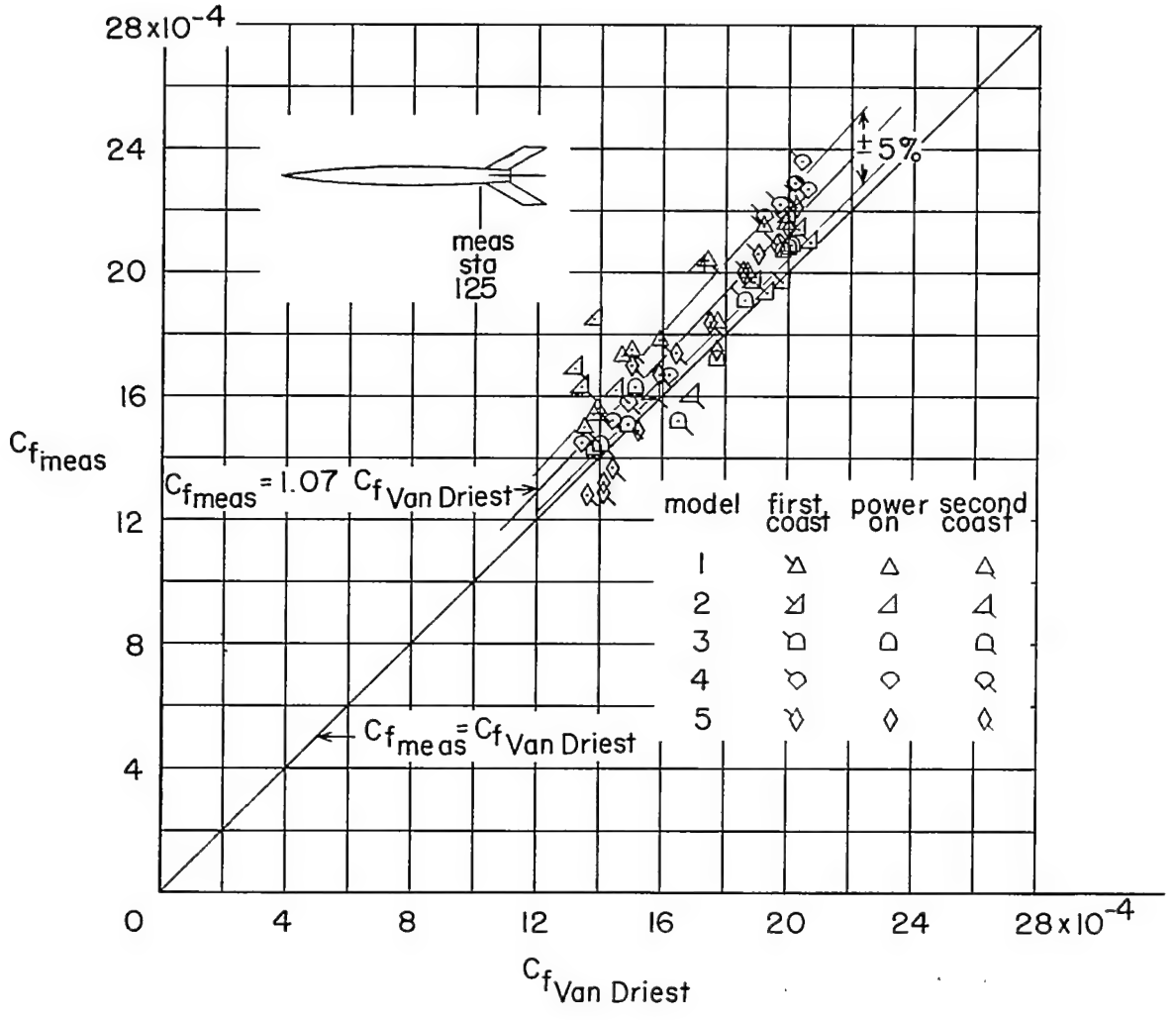

Figure 8.- Comparison of $C_{f_{meas}}$ with $C_{f_{Van\ Driest}}$. Rake station, 125.

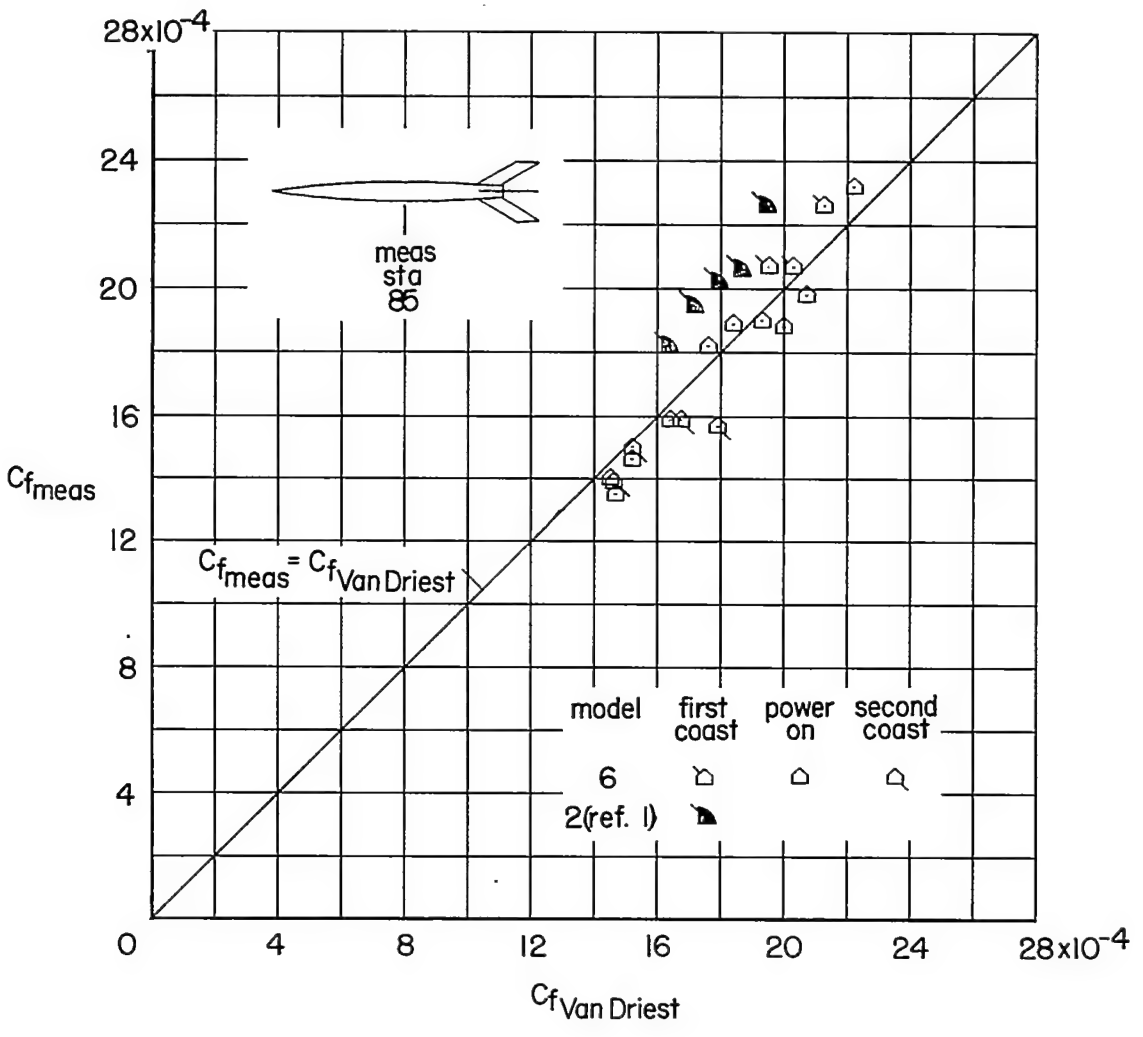

Figure 9.- Comparison of $C_{f_{meas}}$ with $C_{f_{Van\ Driest}}$. Rake station, 85.

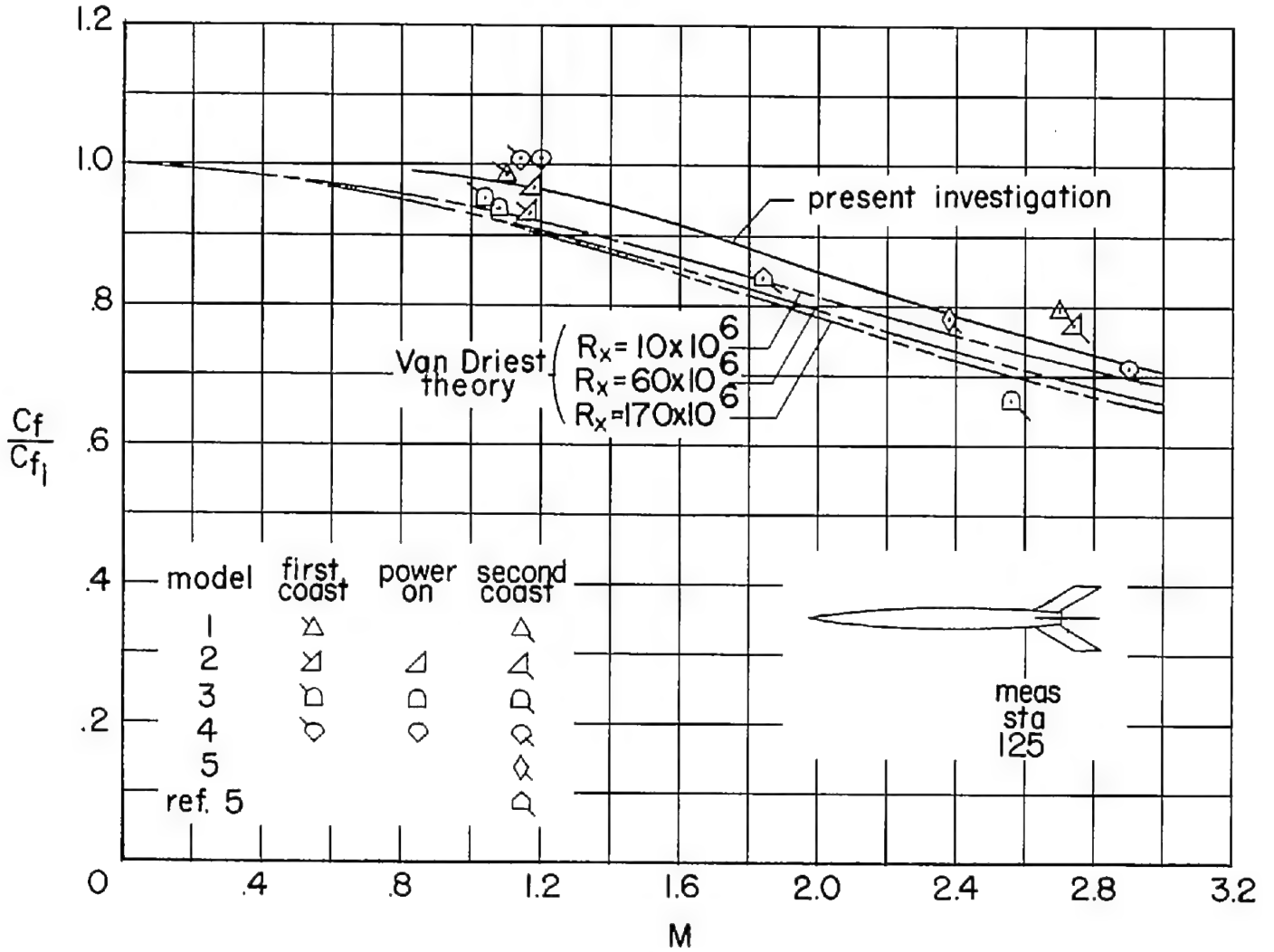

Figure 10.- Ratio of skin friction to incompressible skin friction plotted against Mach number.

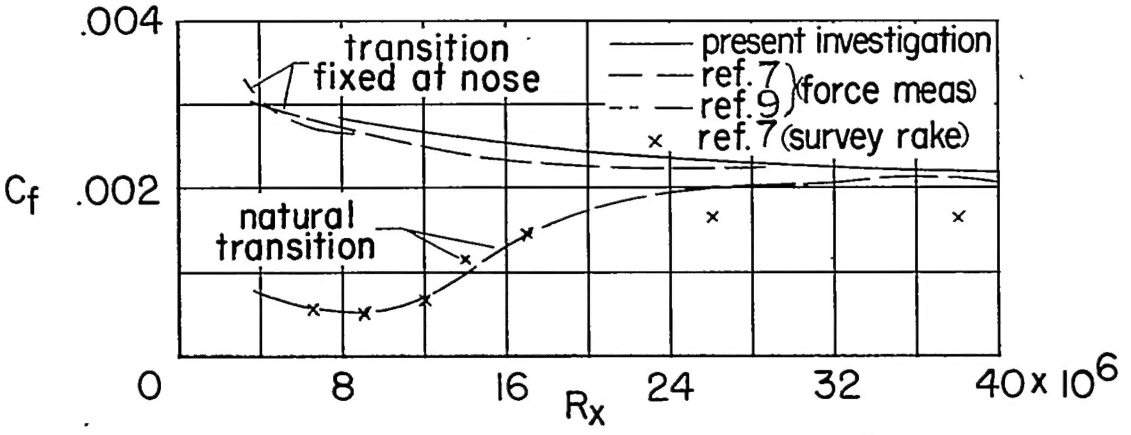

(a) M = 1.6.

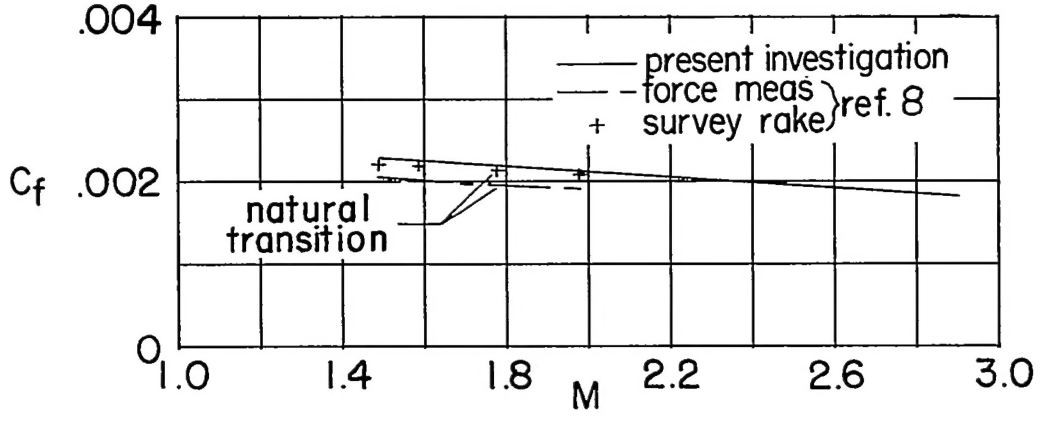

(b) $R_x \approx 30 \times 10^6$.

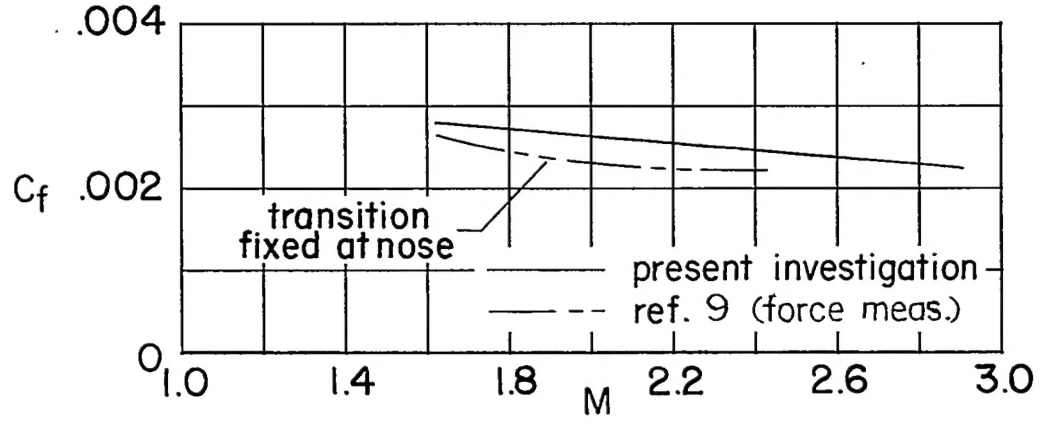

(c) $R_x = 8.5 \times 10^6$.

Figure 11.- Extension of present data compared with tunnel measurements.

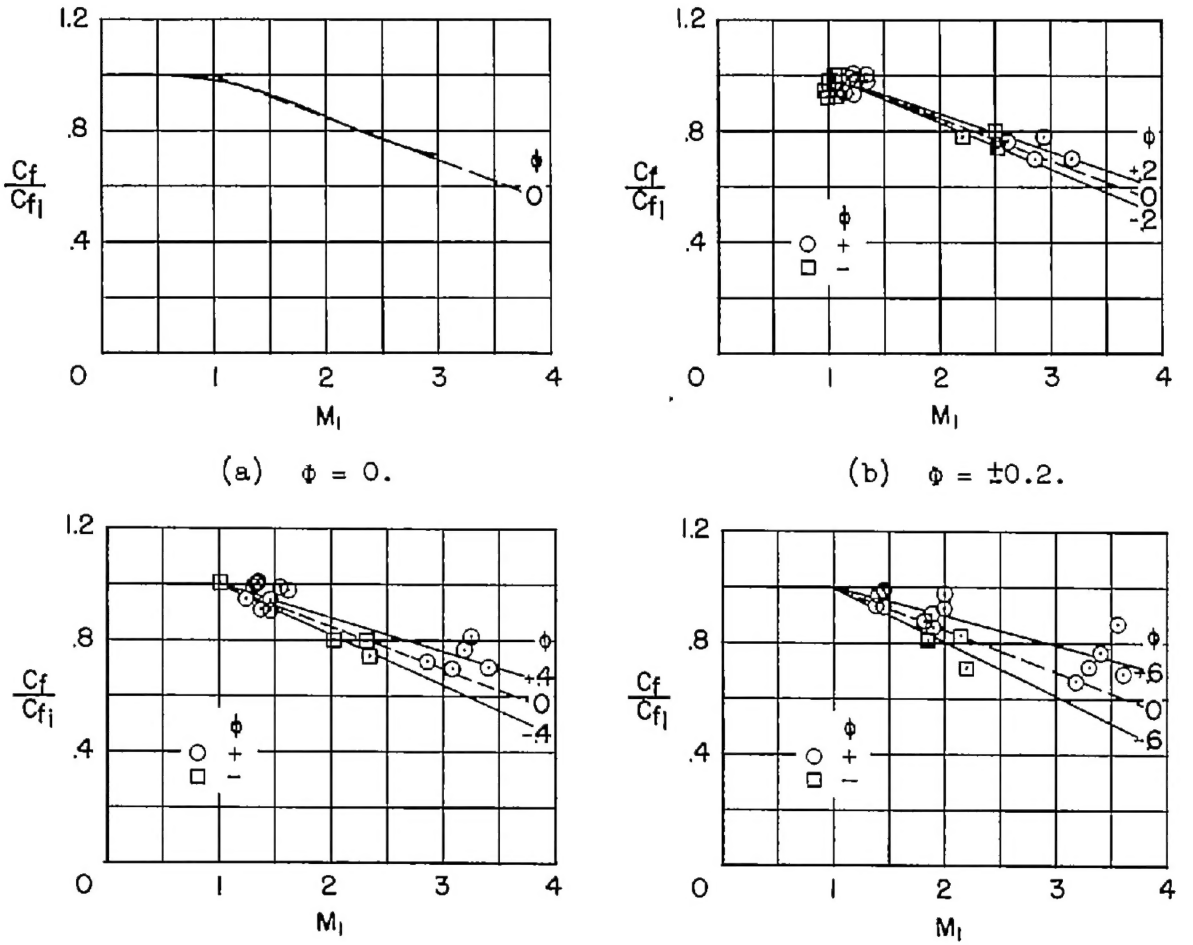

(a) $\Phi = 0.$

(b) $\Phi = \pm 0.2.$

(c) $\Phi = \pm 0.4.$

(d) $\Phi = \pm 0.6.$

Figure 12.- C_f/C_{f_i} for various heating conditions.

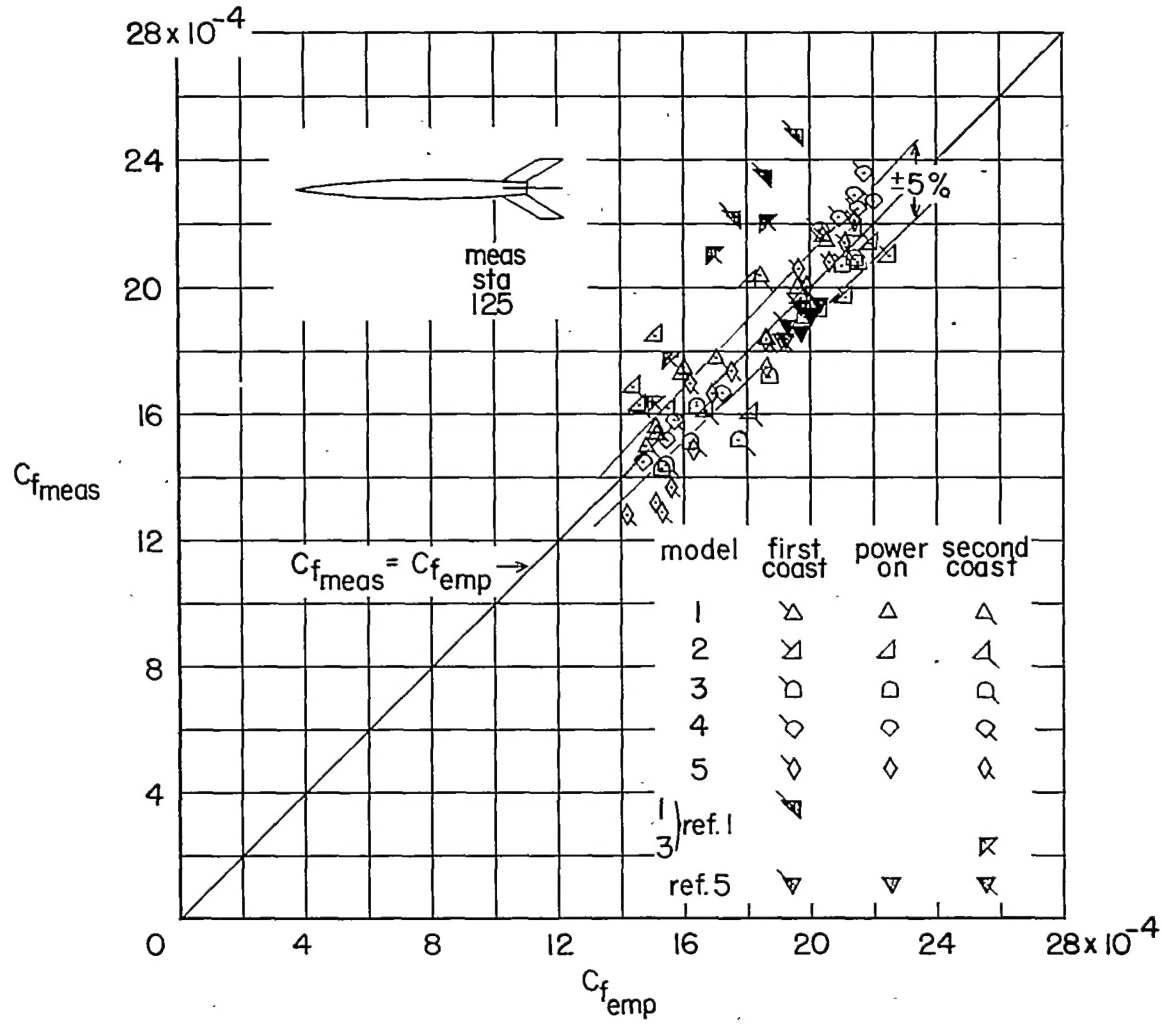

Figure 13.- Comparison of $C_{f_{meas}}$ with $C_{f_{emp}}$.

[redacted]

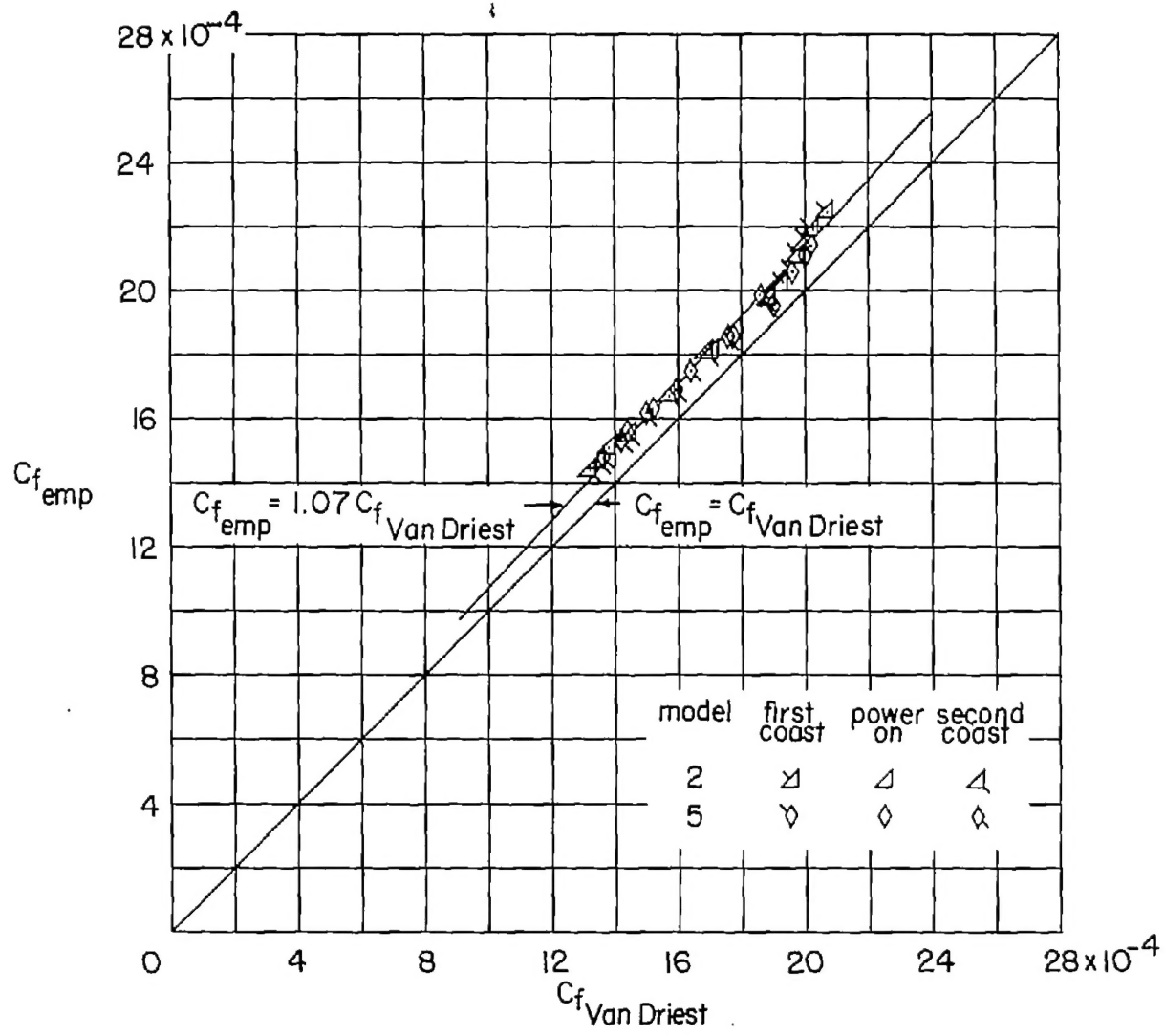

Figure 14.- Comparison of $C_{f_{emp}}$ with $C_{f_{Van\ Driest}}$.